

Utilising implanted carbon fibre as a resistive heating element in wind turbine blade anti-icing systems

A. Maheri

Faculty of Engineering and Environment, Northumbria University, UK

Abstract

Wind turbines installed in cold climates are at risk of blade icing and required to be equipped with systems preventing the build-up of ice and/or ice removal. This paper presents the results of a preliminary investigation on the feasibility and suitability of using carbon fibres as resistive heating elements implanted in the structure of the composite blades. The proof of the concept of using carbon fibre implanted in a glass fibre composite as heating elements for de-icing purpose is demonstrated. Moreover, using a genetic algorithm (GA) optimiser the optimum depth of implanted carbon fibres and the optimum magnitude of heat source which minimise the energy consumption of the system whilst subjected to manufacturing and controllability constraints are obtained. A finite difference model has been also developed to perform the transient heat transfer analysis which is to be used as the evaluator for the optimiser module. The effect of heated fibres on the fibre-matrix debonding strength is also examined. It is shown that, heating the carbon fibres up to 95°C does not affect the fibre-matrix debonding strength. However, the rupture of the carbon fibre tows uncovered in the polymer matrix is the dominant failure mode.

Keywords: wind turbine, blade icing, resistive heating de-icing, resistive heating ant-icing, carbon fibre, GA optimisation, fibre-matrix de-bonding strength.

1 Introduction

The increasing demand for wind energy has led to more wind turbines being deployed in remote areas, many of which are subjected to extreme cold temperatures. It is estimated that wind power generation in 2010 in cold climate locations is approximately 20% of the installed capacity [1]. At colder



temperatures air has a considerably higher density. Hence there is more power available for conversion. However, wind turbines installed in cold climates are at risk of blade icing for large parts of the year. Laakso *et al.* [1] calculated an estimated cost for wind turbine energy loss due to icing and showed that it can reduce the energy yield between 15–25% for a period of icing between 30 and 60 days of the year.

Additional problems caused by ice include the reduced fatigue life, changed natural frequencies and consequently the risk of flutter instability, and potential threat to human safety and damage to nearby structures due to projected ice. The factors which directly influence the fatigue life are asymmetric masses causing rotor unbalance and increased edgewise bending moment fluctuation amplitude due to ice accretion [2].

Many manufacturers are already applying measures to help prevent the build-up of ice (anti-icing) or ice removal (de-icing) by using specially engineered rotor blade coatings, microwave emitters and resistive heating. A resistive heating anti-icing system uses electrical power to heat elements at regular intervals such that the surface temperature is maintained at a level which prevents ice formation and adhesion. A de-icing system, on the other hand, will only be activated at a point when a certain amount of ice has accumulated on the surface of the rotor blade. De-icing includes an inherent downtime for the wind turbine but an anti-icing system does not. The cost effectiveness of either type depends on the energy consumption of the system and the power loss due to wind turbine downtime.

Copper wires and graphite sheets are the most popular resistive heating elements employed in wind turbine blades. Systems using implanted copper wires have the problem of scaling up to MW wind turbines. Systems using graphite sheet fitted to the leading edge are an aftermarket solution and add weight to the blade.

The current composition for most modern wind turbine blades is either epoxy or polyester matrix composites reinforced with glass and/or carbon fibres. Due to monetary reasons however the majority of modern turbine blades are made from glass fibres, although epoxy with carbon fibres has superior mechanical properties with higher strength and stiffness. Another less conventional application of carbon fibre is to use it for its electrical properties [3]. Carbon fibres are supplied in a variety of different forms, from continuous filament tows to short chopped fibres and mats. Tows of continuous filament contain thousands of individual filaments of carbon fibre. These tows can be woven into fabrics which can then be used to reinforce polymers in a composite. The highest strength for a carbon fibre composite is obtained by using unidirectional continuous reinforcement, with the strength lying in the direction of the continuous fibres.

This paper, firstly, demonstrates the proof of concept of using carbon fibre implanted in a glass fibre composite as heating elements for de-icing purpose. Secondly, using a GA the optimum depth and the optimum heating power of carbon fibres as heating elements for a typical wind turbine blade at a general span location are obtained. Finally, the effect of implanted carbon fibres as

heating elements on the fibre-matrix debonding strength of the composite specimen is examined.

2 Resistive heating using carbon fibres, de-icing

The specimen shown in Figure 1 is made of 4 layers of $\pm 45^\circ$ glass fibre epoxy embedding a fifth layer of five tow of carbon fibre located at about 20mm spacing at angle 0. A K-type thermocouple was placed with the measurement junction resting on the middle carbon fibre tow. Both ends of each tow are covered by a conductive silver paint.

The thermogram of Figure 1(b) shows a temperature rise across the whole composite when connected to a source of DC power, but as anticipated the highest temperatures are directly above the heating elements.

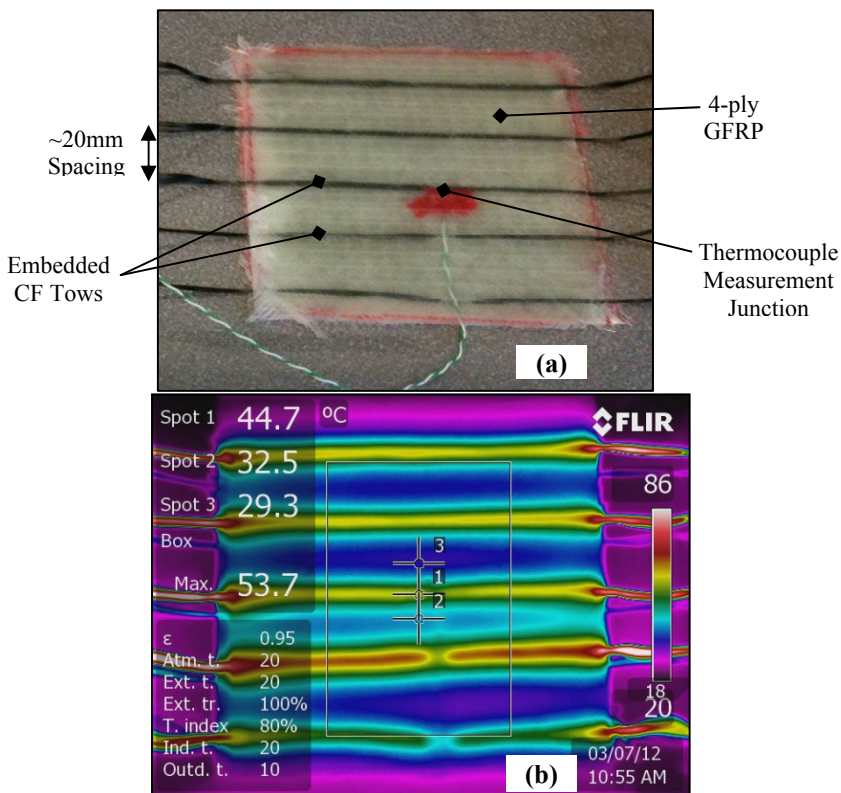


Figure 1: (a) Specimen with carbon fibre tows as heating elements, (b) thermogram.

In order to evaluate the effectiveness of the embedded carbon fibre heating elements at de-icing of the surface of the composite material, the specimen was merged in water and was frozen at -15°C (Figure 2(a)) with an ice thickness of

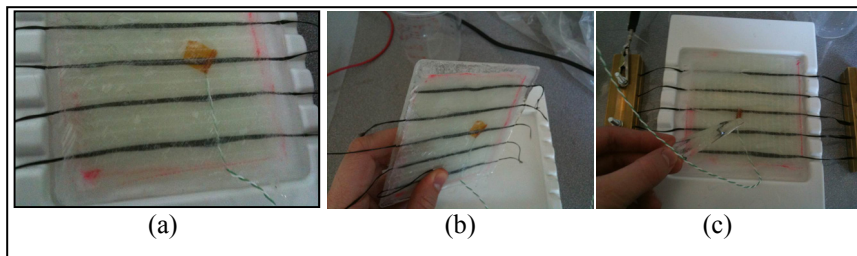


Figure 2: De-icing using implanted carbon fibres.

approximately 3 mm each side (Figure 2(b)). After the start of de-icing process the ice started to come off after approximately 9 minutes (Figure 3(c)).

3 Performance optimisation, anti-icing

Figure 3 shows the cross-section of a typical wind turbine blade rotating with an angular speed of Ω and the coordinate systems $n-s-r$ and $x-y-r$, where r is the radial location along the blade span.

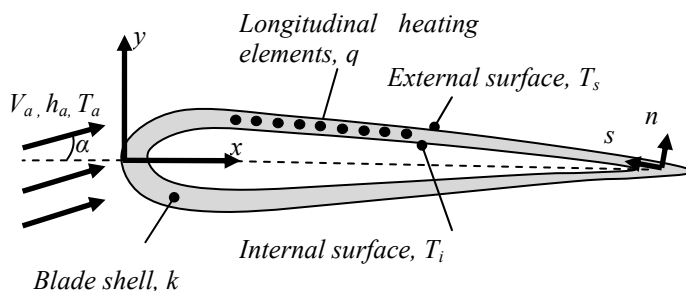


Figure 3: Implanted heating elements in wind turbine blade.

In this figure, $V_a = \sqrt{V_w^2 + r\Omega^2}$ is the relative velocity seen by the blade at a general radial location r , V_w is wind speed, h_a and T_a are the air convection heat transfer coefficient and temperature respectively, α is the angle of attack (AOA), T_i and T_s are the internal and external shell surface temperature respectively, and k stands for the blade shell conductive heat transfer coefficient.

In developing the heat transfer model the following assumptions are made:

- The heat transfer along s axis is neglected. This assumption is valid if the distance between the heat sources (carbon fibres) distributed along s axis is small and the strength of each heat source is controllable independently.

- The heat transfer along r axis is neglected. Although the relative air velocity seen by the blade and consequently the convective heat transfer coefficient depend on the span location, modular design of heating elements along the r axis makes it possible to control the strength of each module proportional to heat transfer rate, keeping the temperature distribution along the blade span uniform.
- Wind speed, rotor speed and consequently the AOA remain constant for the duration of the transient heat transfer analysis.
- The internal surface of the wind turbine blade is assumed to be fully insulated. Therefore the heat loss due to natural convection is assumed to be zero. The validity of this assumption depends on the position of the heating elements and the shell thickness. Using ANSYS based on a heat flux of $q = 1500 \text{ W} / \text{m}^2$, the predicted steady state surface temperatures found for the steady state external surface temperature achieved for the insulated and natural convection scenarios were 46.16°C and 49.32°C for the natural convection and insulated internal surfaces cases respectively. This shows about 6% over-prediction when the internal surface is assumed to be insulated. This error reduces as the shell thickness increases and the heat source is positioned closer to the blade surface. Table 2 shows the rest of the parameters used for this analysis.

Taking into account the effect of the AOA, Wang *et al.* [4] correlated the experimental data with respect to the Nusselt and Reynolds numbers as follows:

$$Nu_x = 0.0943(C_1 + D_1\alpha)Re_c^{0.636} Pr^{1/3} \quad \text{for } Re_c > 5 \times 10^5 \quad (1)$$

$$Nu_x = 2.482(C_1 + D_2\alpha)Re_c^{0.389} Pr^{1/3} \quad \text{for } Re_c \leq 5 \times 10^5 \quad (2)$$

where Re_c represents the chord length specific Reynolds number, $C_1 = 1$ for zero AOA and $C_1 = 0.75$ for non-zero AOA, $D_1 = \pi / 180$ and $D_2 = C_1 D_1$.

Using finite difference methods, the one-dimensional transient heat transfer model was coded in MATLAB. Commercial packages such as ANSYS are suitable for providing solutions for problems with a single set of inputs. However they are not efficient as an evaluation module within an optimisation process, in which design variables, and control parameters are changed through an iterative search algorithm. The purpose of the developed module in MATLAB is to provide efficient evaluation of design candidates during the optimisation procedure. Figure 4 shows the external surface temperature as a function of time obtained by the evaluator module and the results obtained by ANSYS. The data used are as shown in Table 1. A heat flux of $q = 3000 \text{ W} / \text{m}^2$ was used. In the evaluator module a time step of 0.1 second was used.

It can be seen from Figure 4 that the surface temperature reached steady state at 76.62°C when using the evaluator module coded in MATLAB against 76.61°C when ANSYS is employed. This figure shows an excellent agreement with the results obtained by the two software tools with a difference of less than 0.02%.

Table 1: Problem settings.

Parameter	Value
Radial location, r	9.5 m
Rotor speed, Ω	50 rpm
Wind speed, V_w	15 m/s
Angle of attack, α	10°
Matrix initial temperature, T_i	1°C
Initial internal cavity temperature, T_i	1°C
Ambient temperature, T_a	-20°C
Air heat capacity, $c_{p,a}$	1005 J/kgK
Air thermal conductivity, k_a	0.023W/mK
Shell thickness, h	10 mm
Chord length, C	1 m
Heat source depth, h_q	2 mm
Shell heat capacity matrix, $c_{p,m}$	960 J/kgK
Shell thermal conductivity, k_m	0.5 W/mK
Shell density	1800 kg/ m ³

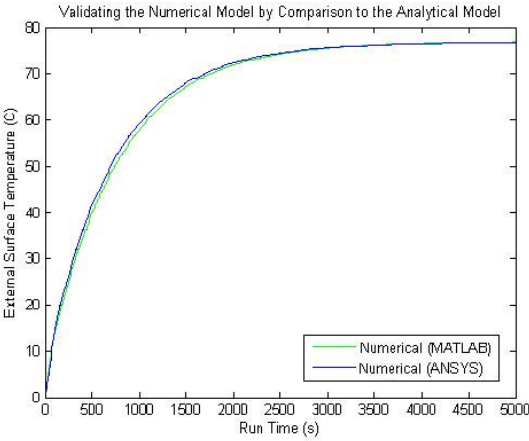


Figure 4: Validation of the developed evaluator module against ANSYS package.

3.1 Optimisation model

3.1.1 Design qualities and design variables

The first stage of the optimisation process is to identify the design qualities of the system. In this instance there are four main qualities to consider: Energy consumption, capital cost, maintenance cost and the system controllability.



The energy consumption is proportional to the power required to heat the surface. The capital costs are a function of material selection, material volume, and design for manufacture. Process control can be controlled by adding restraints at the design stage. Response time, number of activations, and nodal temperature control limits are all examples of process control.

Since the proposed anti-icing system is at conceptual design phase, energy consumption is chosen as the primary objective for the feasibility study while parameters corresponding to the system controllability are treated as constraints.

Here the design variables are the depth of the heat source below the surface h_q , and its strength, q .

3.1.2 Objective and constraints

A time period of 1 hour is chosen to allow compensation for variation in energy consumed during the start-up period. The objective function for energy consumed at a specific location is given by:

$$E = \int_0^{3600} q_i dt \quad (3)$$

In order to avoid the risk of de-lamination or reducing the structural strength of the composite material due to the thermal stresses and the thermal fatigue, the maximum nodal temperature at any location within the blade material is limited to 20°C.

To ensure the system operates as an anti-icing system capable of preventing ice build-up, the external surface temperature is constrained between 3°C and 4°C. The heat source is to be activated when the external surface temperature drops below 3°C and de-activates when the upper limit of 4°C is reached. The response time for the surface to reach the chosen temperature, the overshoot temperature, and the number of activations are three parameters affecting the performance and controllability of the system. The overshoot temperature is defined as the temperature that the system is permitted to reach beyond the upper and lower surface temperature limits.

While the heat flux mainly affects the response time and the overshoot temperature, the depth of the heat source has significant influence on the number of activations (Figure 5).

The heat flux tests illustrated in Figures 5(a) and 5(b) show that the system has a start-up response time of 41 seconds for a heat flux of $q = 1000\text{W/m}^2$, compared to 17 seconds with a $q = 2000\text{W/m}^2$ heat flux. The latent heat energy stored within the matrix material could be responsible for the increase in overshoot temperature when the greater heat flux is applied. Furthermore, the time taken from activation to de-activation of the power source once the system has stabilised is 15 seconds for the 1000W/m^2 system and 8 seconds for the 2000W/m^2 system. This indicates that although the power supplied is increased by a factor of 2, the 'on time' required for the system to maintain the set temperatures is decreased.

Figures 5(a) and 5(c) show that the number of activations is reduced from 20 to 8 by locating the heat source at a depth of 4mm. This can be justified by Fourier's Law and observing that at a greater depth, a greater proportion of the

heat is directed away from the external surface and serves to provide the system with latent heat. When the heat source is located at a distance further from the external surface it is evident that more latent heat is stored within the matrix. When the latent heat is added to the supplied heat it results in a greater overshoot temperature which decreases the level of control over the system.

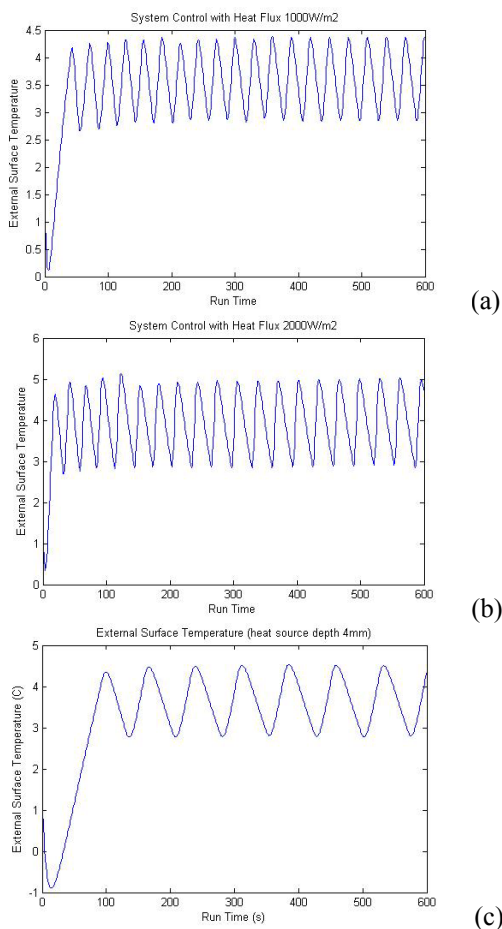


Figure 5: Surface temperature for (a) $h_q = 2\text{mm}$ and $q = 1000\text{W/m}^2$; (b) $h_q = 2\text{mm}$ and $q = 2000\text{W/m}^2$; and (c) $h_q = 4\text{mm}$ and $q = 1000\text{W/m}^2$.

The response time, overshoot temperature and the number of activations are not independent parameters. Figure 6 shows the relationship between the number of activations and the response time. The relationship between response time and the overshoot temperature is also plotted in Figure 6. These results are corresponding to various heat flux values located at a depth of $h_q = 2\text{mm}$. The

results in Figure 6 show that the relationship between the response and number of activations is inversely linear. According to this figure it is not possible to achieve a reduction in response time and a reduced number of activations simultaneously. A reduction in response time produces the undesired result of a system with a higher number of activations.

Figure 6 shows that a response time reduction from 300 seconds to 100 seconds does not yield a large increase in overshoot temperature. However, as the response time is reduced below 60 seconds, the over-shoot temperature increases rapidly.

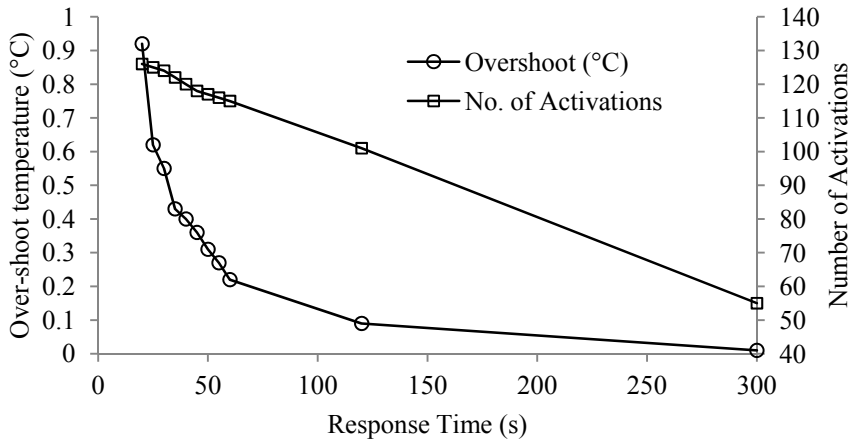


Figure 6: Number of activation and overshoot temperature versus response time.

Since not all control qualities can be achieved simultaneously, in view of Figure 6 a maximum response time of 60 seconds and a maximum overshoot temperature of 0.5°C is used for this study.

3.1.3 Genetic algorithm optimisation

The initial population is generated randomly between limits that are set based on observations of the results from the initial investigation of the finite difference model. A real number encoding is used with standard mutation and arithmetic crossover operators. The infeasible solutions obtained by crossover and mutation operators are rejected. The fitness is defined as:

$$fitness = 1 / \int_0^{3600} q_i dt \quad (4)$$

Using probability of crossover of 0.7, probability of mutation of 0.2 and a population size of 50, the optimum design variables obtained are: heat flux = 837W/m^2 at a location of 2 mm, which was the closest node to the surface. The results shown in Figure 7 give a maximum fitness of $fitness = 7.42 \times 10^{-4}$ equivalent to an energy consumption of $E = 1.35\text{kJ/m}^2$. This is the energy required to maintain the surface temperature within the chosen limits.

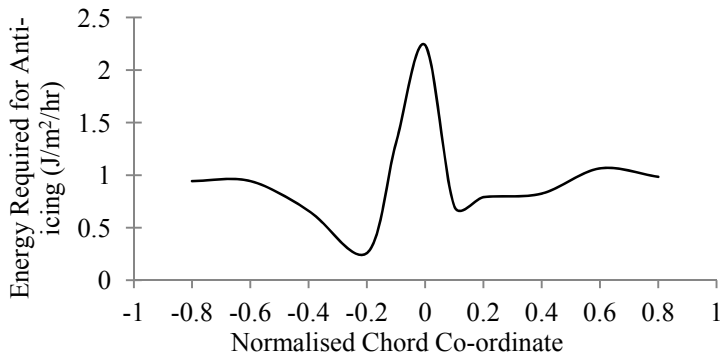


Figure 7: Energy required at normalised chord coordinates.

4 Structural integrity

Heated fibres within a polymer matrix—depending on the severity of heating, the length of the heating period and its variation trend—potentially may lead to fibre-matrix debonding and/or changes in fibre and matrix strengths and therefore an accelerated normal failure mode (delamination, fibre breakage, etc). While the effect of cyclic heating on the overall structural integrity of the blade needs comprehensive experimentations, in this paper the effect of heated fibres on the fibre-matrix debonding strength is examined. Figure 8 shows the test rig employed to measure the ultimate load leading to the breakage of the free fibre tows (uncovered by matrix). It was found that without heating, the uncovered fibres start breaking at a total force of about 280 N. Experiment was repeated by loading a similar specimen up to 260 N (close to the ultimate load) and then

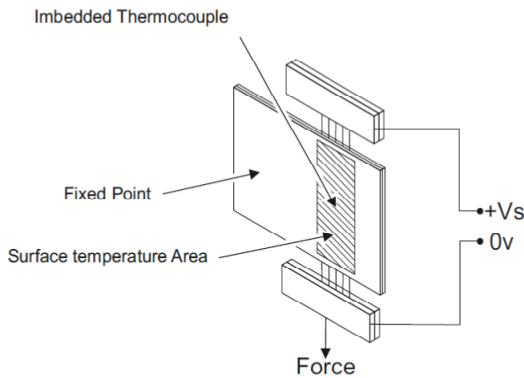


Figure 8: Schematic diagram of the test rig employed to measure the ultimate load leading to the breakage of the free fibre tows (uncovered by matrix).

the temperature of the fibre started to rise incrementally (about 5°C) to a maximum of 95°C (Figure 9). After each temperature rise, the temperature of the fibre was kept constant for about 30 minutes. No fibre-matrix debonding was observed during heating process. Increasing the force to 280 N again led to the breakage of the uncovered fibre. That is, while heating the carbon fibres up to 95°C does not affect the fibre-matrix debonding strength, the rupture of the uncovered fibre is the dominant failure mode.

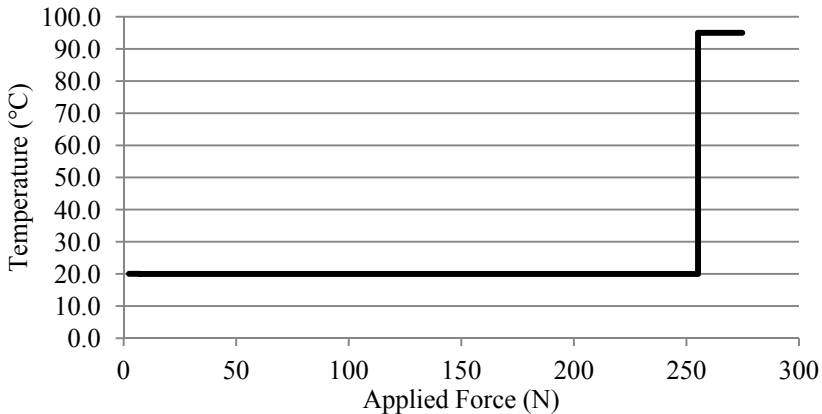


Figure 9: Incremental rise of fibre temperature and applied force.

5 Summary and conclusions

The proof of the concept of using carbon fibres implanted in a glass fibre composite as heating elements for de-icing and anti-icing systems was demonstrated. Employing a genetic algorithm optimisation tool with a one-dimensional finite difference heat transfer code, the optimum depth and the optimum heating power of the implanted carbon fibres for a typical wind turbine blade at a general span location were obtained. A parametric study was carried out to find the relationships between the system control factors. The genetic algorithm optimiser module was set with constraints chosen from the observations in the parametric study. Functioning as an anti-icing system, it was observed that the response time should be maintained above 60 seconds to prevent high overshoot temperatures. It was also showed that an increase in the heat source depth impacts the control of the system adversely because of an increase in the overshoot temperature. Similarly, an increase in the heat flux yields a significant increase in the overshoot temperature and the number of system activations. However, the response time decreases when the heat flux is increased. Finally, the effect of implanted carbon fibres as heating elements on the fibre-matrix debonding strength of the composite specimen was examined. It was shown, while heating the carbon fibres up to 95°C does not affect the fibre-

matrix debonding strength, the rapture of the uncovered fibre is the dominant failure mode.

Acknowledgements

The author would like to thank the Northumbria University graduates Dale Whitehead, Benjamin Smith and James Brooke for their contribution to this research.

References

- [1] Laakso, T., Talhaug, L., Vindteknik, K., Ronsten, G., Horbaty, R., Baring-Gould, I., Lacroix, A., Peltola, E., Wind Energy Projects In Cold Climates, Technical Research Centre, Biologinkuja, 2005.
- [2] Dalili N., Edrisy A. and Carriveau R., A review of surface engineering issues critical to wind turbine performance, Renewable and Sustainable Energy Reviews, 13, pp. 428-438, 2009.
- [3] Athanasopoulos N. and Kostopoulos V., Prediction and experimental validation of the electrical conductivity of dry carbon fiber unidirectional layers, Composites: Part B, 42, 1578-1587, 2011.
- [4] Wang, X., Naterer, GF., Bibeau, E., Convective Heat Transfer From A NACA Airfoil At Varying Angles Of Attack, Journal of Thermophysics and Heat Transfer, 22(3), pp. 457-463, 2008.

